

# UC Irvine

## UC Irvine Previously Published Works

### Title

Steady-state and time resolved fluorescence of albumins interacting with N-oleylethanolamine, a component of the endogenous N-acylethanolamines.

### Permalink

<https://escholarship.org/uc/item/474993xt>

### Journal

Proteins, 40(1)

### ISSN

0887-3585

### Authors

Zolese, G  
Falcioni, G  
Bertoli, E  
[et al.](#)

### Publication Date

2000-07-01

### DOI

10.1002/(sici)1097-0134(20000701)40:1<39::aid-prot60>3.0.co;2-n

### Copyright Information

This work is made available under the terms of a Creative Commons Attribution License, available at <https://creativecommons.org/licenses/by/4.0/>

Peer reviewed

# Steady-State and Time Resolved Fluorescence of Albumins Interacting With N-Oleylethanolamine, a Component of the Endogenous N-Acylethanolamines

Giovanna Zolese,<sup>1\*</sup> Giancarlo Falcioni,<sup>2</sup> Enrico Bertoli,<sup>1</sup> Roberta Galeazzi,<sup>3</sup> Michal Wozniak,<sup>4</sup> Zbigniew Wypych,<sup>4</sup> Enrico Gratton,<sup>5</sup> and Annarina Ambrosini<sup>1</sup>

<sup>1</sup>*Istituto di Biochimica, Facoltà di Medicina e Chirurgia, Università di Ancona, Ancona, Italy*

<sup>2</sup>*Dipartimento di Biologia M.C.A., Camerino, Italy*

<sup>3</sup>*Dipartimento Scienze dei materiali e della Terra, Università di Ancona, Ancona, Italy*

<sup>4</sup>*Department of Chemistry, Medical University of Gdansk, Gdansk, Poland*

<sup>5</sup>*Laboratory for Fluorescence Dynamics, University of Illinois, Urbana, Illinois*

**ABSTRACT** The functions of N-acylethanolamines, minor constituents of mammalian cells, are poorly understood. It was suggested that NAEs might have some pharmacological actions and might serve as a cytoprotective response, whether mediated by physical interactions with membranes or enzymes or mediated by activation of cannabinoid receptors. Albumins are identified as the major transport proteins in blood plasma for many compounds including fatty acids, hormones, bilirubin, ions, and many drugs. Moreover, albumin has been used as a model protein in many areas, because of its multifunctional binding properties. Bovine (BSA) and human (HSA) serum albumin are similar in sequence and conformation, but differ for the number of tryptophan residues. This difference can be used to monitor unlike protein domains. Our data suggest that NOEA binds with high affinity to both albumins, modifying their conformational features. In both proteins, NOEA molecules are linked with higher affinity to hydrophobic sites near Trp-214 in HSA or Trp-212 in BSA. Moreover, fluorescence data support the hypothesis of the presence of other NOEA binding sites on BSA, likely affecting Trp-134 environment. The presence of similar binding sites is not measurable on HSA, because it lacks of the second Trp residue. *Proteins* 2000;40:39–48.

© 2000 Wiley-Liss, Inc.

**Key words:** fluorescence; circular dichroism; albumin; N-acylethanolamine

## INTRODUCTION

N-acylphosphatidylethanolamines (NAPEs) and N-acylethanolamines (NAEs) were identified as minor constituents of some mammalian cells and tissues.<sup>1</sup> The physiological significance of these compounds is poorly understood, although many functions was suggested. NAPEs are precursors of NAEs, which can be formed in different circumstances: they can accumulate in conditions involving degenerative changes to tissues, as in brain and cardiac ischemia.<sup>1</sup> Moreover, their synthesis can be stimulated [e.g., by excitatory amino acids (EAAs) in cultured

central neurons].<sup>2</sup> It was suggested that these compounds might have membrane stabilizing effects,<sup>1,3</sup> can protect against lipid peroxidation,<sup>1</sup> and have some pharmacological actions, such as anti-inflammatory effects.<sup>1</sup> Recent works demonstrated that cannabinoid receptors recognize some N-acylethanolamines, suggesting that these compounds are functionally active on mast cells and cerebellar granular cells.<sup>4,5</sup> Moreover, these works suggests that NAEs and NAPEs might serve as a cytoprotective response, whether mediated by physical interactions with membranes or enzymes or mediated by activation of cannabinoid receptors,<sup>6</sup> with possible pathophysiological roles in the brain. Albumins are involved in the maintenance of colloid osmotic blood pressure and were identified as the major transport proteins in blood plasma for many compounds including fatty acids, hormones, bilirubin, ions, and many drugs. Albumins are implicated in the facilitated transfer of many ligands across organ-circulatory interfaces such as in the liver, intestine, kidney, and brain,<sup>7</sup> and the existence of an albumin cell surface receptor was suggested.<sup>8</sup> Human serum albumin (HSA) was long used as a model protein in many areas, as in ligand/drug displacement studies. A large number of studies focused on the multifunctional binding properties of serum albumin. The majority of these drug-binding studies involving serum albumin, showed that the distribution, free concentration and metabolism of many substances can be significantly altered as a function of their binding to this protein.<sup>9</sup> Moreover, ligand binding could affect the structural and dynamic features of albumin, probably modifying its functional characteristics.

Bovine serum albumin (BSA) (583 aa) and HSA (585 aa) are characterized by an high homology in the sequence

*Abbreviations:* NAPEs, N-acylphosphatidylethanolamines; NAEs, N-acylethanolamines; HSA, human serum albumin; BSA, bovine serum albumin; ANS, 1-anilinonaphtalene-8-sulfonic acid.

Grant sponsors: M.U.R.S.T. and C.N.R.

\*Correspondence to: Dr. Giovanna Zolese, Istituto di Biochimica, Facoltà di Medicina e Chirurgia, Via Ranieri, 60131 Ancona, Italy. E-mail: zolese@popcsi.unian.it

Received 14 May 1999; Accepted 6 January 2000

(80%) and similar conformation, containing 17 disulfide bridges and a series of nine loops, assembled in three domains (I, II, III), each formed by two subdomains, A and B.<sup>10</sup> The principal binding regions are located in subdomains IIA and IIIA<sup>10</sup> and it is generally assumed that in BSA and HSA these sites are homologous, although they may differ in affinity.<sup>10</sup> The structure of HSA was recently determined by X-ray crystallography.<sup>11</sup> In this protein the single Trp residue (Trp-214) is located in IIA binding site, where Lys-199 and His-242 are involved in the protein-ligand interaction. Trp-214 plays an important structural role by limiting the solvent accessibility.<sup>11</sup> Moreover, this amino acid participates in an hydrophobic packing interaction between IIA and IIIA interface.<sup>11</sup> It was demonstrated that the domains are assembled to form an heart-shaped molecule.<sup>11</sup> However, the assembling of the domains can be modified depending on the conditions (as e.g., pH).<sup>10</sup> In addition, from the comparison of many fluorescence anisotropy decay data for Trp-214 in HSA, it was concluded<sup>12</sup> that the protein can easily adopt many conformations, ranging from a more compact form to a more extended form (e.g., as a consequence of temperature changes). BSA is characterized by two Tryptophanyl residues: Trp-212 is thought to be located in a similar hydrophobic microenvironment as the single Trp-214 in HSA (subdomain IIA),<sup>10</sup> whereas Trp-134 is considered to be more exposed to solvent and it is localized in subdomain IA. Previous works demonstrated that 63% of BSA fluorescence emission ( $\lambda_{\text{ex}} = 295 \text{ nm}$ ) is linked to Trp-134. The fluorescence features of Trp in both albumins are used to study ligand binding to these proteins.<sup>13,14</sup> Because Trp-214 in HSA and Trp-212 in BSA are located in sites with similar characteristics and highly homologous in sequence, it is considered that these amino acids can show similar fluorescence behavior as consequence of ligand binding in their environments.<sup>13,14</sup>

The aim of this work is to study the interaction of NAEs with HSA and BSA. In particular, we studied N-oleylethanolamine (NOEA) which was shown to protect against increased  $\text{Ca}^{2+}$  permeability of isolated damaged mitochondria<sup>1</sup> and to be an inhibitor of ceramidase and ceramide can induce apoptosis<sup>6</sup> (and references cited therein). The chemical characteristics of NAEs suggest the possibility that their primary action could be played on the lipidic part of the membrane. However, there is the possibility that properly tailored binding sites may exist on proteins to accommodate the long hydrophobic chain of NAEs. The possible interaction of these molecules with serum albumin and the possible modifications induced on structural and motional properties of this protein could be of interest as a possible model of their interaction with proteins and for implications in the transport and availability of this endogenous class of lipids to tissues. Steady-state and time-resolved fluorescence studies were used to compare the effect of NOEA on albumins. Fluorescence data were correlated with circular dichroism data.

## MATERIALS AND METHODS

Fatty acid-free human serum albumin (HSA) (Sigma A-1887) and fatty acid-free bovine serum albumin (BSA)

(Sigma A-0281) were used without further purification. 1-anilino-naphthalene-8-sulfonic acid (ANS) was purchased from Molecular Probes. N-oleylethanolamine (NOEA) was synthesized as previously described.<sup>3</sup> NOEA stock solutions were made in ethanol, immediately before use. In each experiment, no more than 2  $\mu\text{l}$  of ethanol was used. Control experiments, performed with the same amount of solvent, demonstrated that it had no effect on HSA and BSA, at the amounts used in this work, in each technique used.

## Steady-State Fluorescence Measurements

Steady-state fluorescence measurements of intrinsic HSA and BSA fluorescence were performed by a Perkin-Elmer LS50 B, using an excitation wavelength of 295 nm. Final protein concentration was 190  $\mu\text{g/ml}$ , in 20 mM Tris/HCl, 0.1 mM EDTA, and 150 mM NaCl. Data were acquired at 37°C. Samples were equilibrated at the temperature used for 10 min before data acquisition. In ANS experiments, two excitation wavelengths were used: 350 nm and 295 nm. ANS final concentration was 1.8  $\mu\text{M}$ , the protein concentration was 190  $\mu\text{g/ml}$ . Data presented are the average of at least three different experiments. All spectra were corrected for scatter by subtracting the baseline of proper buffer solutions measured with the same instrumental conditions.

## Time-Resolved Fluorescence Measurements

The decay of albumins was studied by a multifrequency phase fluorometer, at the Laboratory for Fluorescence Dynamics (LFD), University of Illinois at Urbana-Champaign (USA), using the harmonic content of a Coherent Nd:YAG mode-locked laser pumping a rhodamine dye laser. Excitation was at 295 nm using magic angle configuration, and the emission was observed through a Schott WG-320 filter to isolate the emission of tryptophan and block-scattered light. A solution of p-terphenyl in ethanol (lifetime 1.05 ns) was used as reference. The modulation frequency was varied from 3.81 to 350.52 MHz. Data were acquired at 15 different frequencies with the uncertainties of 0.2° and 0.004 for phase angles and modulation ratios respectively. Anisotropy decay data were acquired with the same set of frequencies, using an excitation wavelength 295 nm. Fluorescence decay data were fitted to a sum of exponential decay components using a nonlinear least square analysis or as continuous distributions of lifetime values. Data were analyzed using Globals Unlimited software, according to models and equations described by Alcalá et al.<sup>15</sup> The reduced  $\chi^2$  value was used to judge the goodness of fit.<sup>15</sup> All measurements were performed at 37°C. Final protein concentration was 190  $\mu\text{g/ml}$ , NOEA was 4.8  $\mu\text{M}$  (NOEA/albumin molar ratio =  $R = 1.65$ ). Data are means of three to six different experiments.

## Circular Dichroism (CD)

Near-UV (from 320 nm to 260 nm) and Far-UV CD spectra (from 260 to 200 nm) were recorded on a Jasco 500 spectropolarimeter under constant Nitrogen flux, at 37°C. The instrument was calibrated with a solution of pantolac-

tone 0.015%. For the standard solution a 1-cm path-length cell was used and spectra scanned at 50 nm/min with a time constant of 1 sec. In Far-UV region, for protein samples the path length was 0.2 mm with an accumulation of five scans, for each experiment. Both proteins concentration was 160  $\mu\text{g/ml}$ . In the Near-UV region, a pathlength of 1 cm was used, and protein concentration was 1.3 mg/ml. NOEA was added to samples up to a NOEA/protein molar ratio 7.5/1. In the case of near UV CD, NOEA  $\mu\text{molar}$  concentrations were necessarily higher than those used in the other CD range, to obtain similar NOEA/protein molar ratios. Readings were done against a reference cuvette containing the same components, except the protein. Data were the average of five individual spectra.

### 3D-Space-Filling Modeling

To perform the molecular docking to the HSA binding site, Monte Carlo methods were used, in conjunction with simulated annealing.<sup>16</sup> At each iteration of the MC procedure, the internal conformation of the ligand is changed, the energy of the ligand within the binding site is calculated using molecular mechanics and, particularly, by using AMBER force field<sup>17</sup> as implemented in MacroModel v.5.5<sup>18</sup> and HyperChem 4.6 for SGI (HyperChem 4.6, SGI version, Hypercube Inc., Ontario, Canada). All the calculations were performed on an Indigo2 SGI Workstation R10000 175 MHz and on a SGI Workstation O2 R10000 195 MHz.

The significance of the data obtained in each kind of experiment was calculated according to Student's *t*-test.

## RESULTS

### Steady-State Fluorescence of Tryptophan

The intrinsic fluorescence of Trp residues present in Human and Bovine albumins was used for this work. Preliminary studies were performed to evaluate the possibility of Trp quenching effects by NOEA (up to 35 mM), which was excluded by experiments on Tryptophan octyl ester (12  $\mu\text{M}$ ) in ethanol (data not shown). Figure 1A shows steady-state fluorescence emission spectra for HSA in the presence of increasing concentrations of NOEA. NOEA induces a small decrease of Trp fluorescence intensity (about 6%), although no more changes are evident at concentrations above 6–8  $\mu\text{M}$  ( $R = \text{NOEA/protein molar ratio} = 2\text{--}2.7$ ). The most evident NOEA-induced effect is a blue shift in  $\lambda_{\text{em}}$  visible in each spectrum in Figure 1. This change becomes significant at 3.9  $\mu\text{M}$  NOEA ( $p < 0.01$ ).

Figure 1B shows steady-state fluorescence emission spectra obtained for BSA in the presence of increasing concentrations of NOEA. In these spectra a NOEA-induced intensity decrease (up to 29%) and a blue shift in  $\lambda_{\text{em}}$  can be observed. The intensity decrease is significant at 3.9  $\mu\text{M}$  NOEA ( $p < 0.01$ ), whereas  $\lambda_{\text{em}}$  shift is significant at 6  $\mu\text{M}$  NOEA ( $p < 0.01$ ). Because HSA contains a single Trp at the position 214, which is considered analogous to Trp-212 on BSA<sup>10</sup> and these residues show a similar fluorescence behavior,<sup>13,14</sup> the emission spectrum of HSA was subtracted to BSA spectrum, to disentangle the spectral contribution of Trp-212 and Trp-134. On these

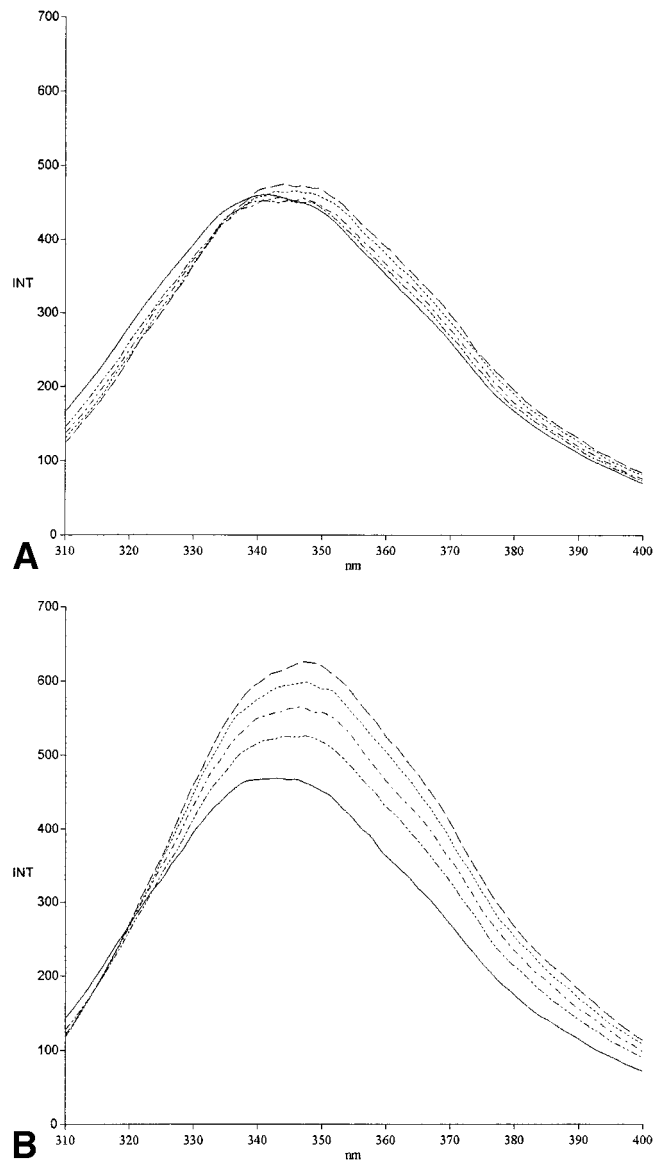


Fig. 1. Fluorescence spectra of HSA (panel A) and BSA (Panel B) in presence of increasing NOEA concentrations: (---) Control; (···) 1.96  $\mu\text{M}$  NOEA; (-·-·-) 3.92  $\mu\text{M}$  NOEA; (·-·-·) 5.88  $\mu\text{M}$  NOEA; (—) 9.79  $\mu\text{M}$  NOEA. Spectra were recorded at 37°C. The excitation wavelength was set at 295 nm (bandwidth 4 nm), and the emission spectra were recorded between 310–400 nm (bandwidth 4 nm). Samples were dissolved in 20 mM Tris, 0.1 mM EDTA, 150 mM NaCl, pH 7.2.

spectra (indicated as BSA-HSA) the calculation of center-of-mass was performed, according to Ehrhardt et al.<sup>19</sup> This parameter was calculated because it is more reproducible than the estimation of spectral maxima. The same calculation was performed on HSA and BSA spectra. Results are presented in Figure 2. From this figure, it is evident that the HSA center-of-mass flattens around 7.8–9.8  $\mu\text{M}$  NOEA (corresponding to a NOEA/protein molar ratio =  $R = 2.7\text{--}3.4$ ). In BSA-HSA spectra, there is a constant value of the center-of-mass up to 7.8  $\mu\text{M}$  NOEA ( $R = 2.7$ ), whereas the increase of this parameter flattens between 11.75  $\mu\text{M}$  and 23.5  $\mu\text{M}$ . The behavior of the BSA curve is intermedi-



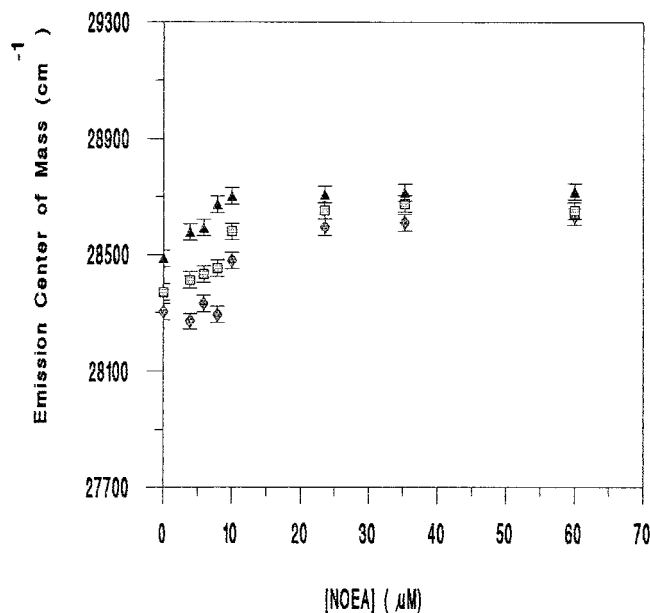


Fig. 2. Effect of increasing NOEA concentrations on the center-of-mass of the fluorescence emission spectra of HSA ( $\Delta$ ), BSA ( $\square$ ) and difference spectra BSA-HSA ( $\blacklozenge$ ). Data were obtained at 37°C with  $\lambda_{\text{ex}} = 295$  nm. Proteins (190  $\mu\text{g}/\text{ml}$ ) were suspended in 20 mM Tris/HCl, 0.1 mM EDTA, 150 mM NaCl, pH 7.3. Data are presented as means of at least three different experiments.

ate between the HSA and BSA-HSA curves (Fig. 2). Although Trp fluorescence is not directly quenched by NOEA, the intensity decrease induced on albumin fluorescence is directly related to the NOEA binding to albumins. For this reason, the fluorescence decrease was used to calculate the affinity of NOEA for its binding sites on the protein. The value of fluorescence intensity was measured at the wavelength corresponding to the frequency of the center-of-mass. The dissociation constant,  $K_d$  was calculated by the formula

$$1/\Delta F = (K_d/\Delta F_{\text{max}})(1/[\text{NOEA}]) + 1/\Delta F_{\text{max}}$$

where  $\Delta F_{\text{max}}$  is the maximum fluorescence change possible in the sample and  $K_d$  is the dissociation constant. The formula was obtained by a modification of the method of Johansson et al.<sup>13</sup> For BSA, the averaged dissociation constant for the NOEA binding sites in the environment of both tryptophans was  $K_d = 2.1 \pm 0.9 \times 10^{-5}$ ,  $K_a = 5.4 \pm 2.5 \times 10^4$ . The same analysis was carried out on HSA: calculated  $K_d$  for HSA was  $K_d = 4.3 \pm 0.7 \times 10^{-6}$ ,  $K_a = 2.4 \pm 0.4 \times 10^5$ . The  $K_d$  and  $K_a$  for Trp-134 of BSA were calculated by BSA-HSA spectra previously described:  $K_d = 2.4 \pm 0.3 \times 10^{-5}$  and  $K_a = 4.3 \pm 0.6 \times 10^4$ . These values indicate that the binding site located near the more exposed Trp-134 is characterized by a lower affinity for NOEA.

### Time-Resolved Fluorescence of Tryptophan

The fluorescence decay measurements for the single Trp of HSA were acquired in the presence and the absence of 4.8  $\mu\text{M}$  NOEA ( $R = 1.65$ ). This not saturating NOEA concentration was chosen to underline the early engaged

albumin domain. In fact, the comparison between HSA and BSA fluorescence can help to understand which part of albumin is early affected by low concentrations of NOEA. At this NOEA concentration, only  $\approx 50\%$  HSA molecules are bound to the ligand. Although the fluorescence and anisotropy decay data arise from a heterogeneous HSA population (bound and unbound molecules), the modifications induced on the measurements are likely because of the NOEA binding on site (or sites) with higher affinity. At higher NOEA concentrations, some binding sites with lower affinity could be occupied partially by ligand, likely affecting other protein domains. The apparent  $K_a$  measured for BSA is an average of strong and weak binding. According to Johansson,<sup>30</sup> it is assumed that the strong affinity constant for BSA is the same as that calculated for HSA and, that a  $\approx 50\%$  saturation is reached in these sites on both proteins. The high homology between BSA and HSA suggests that NOEA binding sites are localized in similar domains. However, the comparison between fluorescence decay data from HSA and BSA can help to exclude the presence of high affinity binding sites in the Trp-134 environment. The results of lifetime analysis are shown in Table I. Using the exponential analysis, the best results were obtained by a three exponential fit, where lifetime components ( $\tau_i$ ) are 6.88 ns, 3.21 ns, and 0.41 ns, with associated fractional intensities ( $f_i$ ) 0.57, 0.36, 0.07, respectively (Table IA). These results are in line with previous data obtained for HSA at a lower temperature (25°C).<sup>20</sup> NOEA induces small but significant ( $p < 0.05$ ) modifications in longer lifetime values (6.40 ns and 2.74 ns, respectively) ( $-7\%$  and  $-15\%$ , respectively), but not in their fractional intensities (Table IIA). Table IB shows results obtained by analyzing the same data in terms of Gaussian distributions of lifetimes, in agreement with Marzola and Gratton.<sup>20</sup> Lorentzian and Uniform distributions did not yield similar good fits in our samples. An increase of fit, without significant changes in the center value, was obtained including a very short lifetime (0.001 ns) in the analysis, to eliminate light scattering contribution<sup>21,22</sup> (Table IB). In the Gaussian distributional analysis a NOEA induced significant decrease in the value of the center of the distribution (from 5.39 ns to 4.92 ns, ( $p < 0.02$ ) can be observed, with no change in the distributional width. In Table II are shown the results obtained analyzing fluorescence decay data for BSA in the presence and the absence of 4.8  $\mu\text{M}$  NOEA ( $R = 1.66$ ). The phase and modulation data are analyzed by using a three-component exponential decay or a Gaussian distribution of lifetimes, because these analyses give analogous fits for the data. Using the exponential analysis, the best results were obtained by a three exponential fit, where lifetime components ( $\tau_i$ ) are 6.50 ns, 3.63 ns, and 0.51 ns, with associated fractional intensities ( $f_i$ ) 0.67, 0.28, 0.05, respectively. NOEA induces very small modifications in longer lifetime values (6.29 ns and 3.16 ns, respectively), but not in their fractional intensities (Table IIA). The same data were analyzed using distributional models (Table IIB). As in the case of HSA, data yielded a slightly improved fit using a Gaussian distributional analysis and including a very

**TABLE I. Fluorescence Decay Fitting Parameters for HSA, in the Presence or the Absence of 4.8  $\mu$ M NOEA ( $R = 1.65$ )<sup>†</sup>**

A	$\tau_1$	$f_1$	$\tau_2$	$f_2$	$\tau_3$	$\chi^2$
HSA	$6.88 \pm 0.16$	$0.57 \pm 0.05$	$3.21 \pm 0.21$	$0.36 \pm 0.04$	$0.41 \pm 0.8$	0.19
+NOEA	$6.40 \pm 0.03^*$	$0.60 \pm 0.02$	$2.74 \pm 0.05^*$	$0.34 \pm 0.02$	$0.35 \pm 0.06$	0.27
B	$c_1$	$w_1$	$f_1$	$c_2$	$w_2$	$\chi^2$
HSA	$5.35 \pm 0.03$	$2.51 \pm 0.03$	1			4.62
	$5.39 \pm 0.02$	$2.06 \pm 0.02$	$0.98 \pm 0.00$	0.001	$0.17 \pm 0.06$	0.18
+NOEA	$4.88 \pm 0.07^{**}$	$2.35 \pm 0.06$	1			1.63
	$4.92 \pm 0.08^{**}$	$2.12 \pm 0.00$	$0.99 \pm 0.00$	0.001	$0.02 \pm 0.02$	0.23

<sup>†</sup>Fluorescence decay was measured at 37°C, with an excitation wavelength of 295 nm. Data were fitted to a sum of exponential decay components (A) or as Gaussian distributions of lifetime values (B).

Data, acquired at 37°C, are presented as mean  $\pm$  SD. Panel A:  $\tau_1, \tau_2, \tau_3$ , lifetime values (ns);  $f_1, f_2, f_3$ , fluorescence fractions,  $f_1 + f_2 + f_3 = 1$ . Panel B:  $c_1, c_2, w_1, w_2$ , centers and widths of Gaussian distributions;  $f_1, f_2$ , fluorescence fractions,  $f_1 + f_2 = 1$ ; in both panels  $\chi^2$ , reduced chi-square.

\* $p < 0.05$ , \*\* $p < 0.02$ . Comparison was made with HSA data analyzed in a similar way.

**TABLE II. Fluorescence Decay Fitting Parameters for BSA, in the Presence or the Absence of 4.8  $\mu$ M NOEA<sup>†</sup>**

A	$\tau_1$	$f_1$	$\tau_2$	$f_2$	$\tau_3$	$\chi^2$
BSA	$6.50 \pm 0.18$	$0.67 \pm 0.05$	$3.63 \pm 0.32$	$0.30 \pm 0.05$	$0.51 \pm 0.10$	0.50
+NOEA	$6.29 \pm 0.09$	$0.67 \pm 0.10$	$3.16 \pm 0.19$	$0.28 \pm 0.07$	$0.54 \pm 0.18$	0.43
B	$c_1$	$w_1$	$f_1$	$c_2$	$w_2$	$\chi^2$
BSA	$5.57 \pm 0.24$	$2.20 \pm 0.16$	1			9.41
	$5.69 \pm 0.06$	$1.34 \pm 0.11$	$0.95 \pm 0.02$	<0.01	$1.43 \pm 0.71$	0.46
+NOEA	$5.27 \pm 0.34$	$2.37 \pm 0.14$	1			7.2
	$5.51 \pm 0.09$	$1.48 \pm 0.07$	$0.90 \pm 0.08$	<0.01	$2.20 \pm 1.39$	0.45

<sup>†</sup>Fluorescence decay was measured at 37°C, with an excitation wavelength of 295 nm. Data were fitted to a sum of exponential decay components (A) or as Gaussian distributions of lifetime values (B).

For symbols, see Table I.

**TABLE III. Anisotropy Decay Parameters for HSA (A) and BSA (B) in the Absence and the Presence of 4.8  $\mu$ M NOEA ( $R = 1.65$ )<sup>†</sup>**

	$\phi_1$ (ns)	$\phi_2$ (ns)	$f_L$	$r_o^a$	$\chi^2$
A					
HSA	$16.7 \pm 1.5$	$0.17 \pm 0.03$	$0.47 \pm 0.01$	0.31	0.197
HSA + NOEA	$16.1 \pm 3.5$	$0.17 \pm 0.05$	$0.45 \pm 0.05$	0.31	0.283
B					
BSA	$15.1 \pm 0.6$	$0.24 \pm 0.02$	$0.41 \pm 0.01$	0.31	0.344
BSA + NOEA	$15.7 \pm 0.6$	$0.21 \pm 0.09$	$0.41 \pm 0.05$	0.31	0.454

<sup>†</sup> $T = 37^\circ\text{C}$ . Data were acquired using a  $\lambda_{\text{ex}} = 295$  nm.

$\phi_1, \phi_2$ , rotational correlation times;  $f_L$  = fraction of anisotropy linked to longer rotational correlation time.<sup>21</sup>

<sup>a</sup> $r_o$  was fixed to 0.31.

short lifetime (0.001 ns) to eliminate light scattering contribution.<sup>21,22</sup> The center of the distribution and the distributional widths are only slightly modified.

In Table III is reported the best fit for anisotropy decay obtained with data of Tables I and II. The anisotropy decay of HSA at 37°C is analyzed using two rotational correlation times, 16.7 ns and 0.17 ns. The limiting anisotropy  $r_o$  was fixed at the experimental value 0.31, obtained for NATA at low temperatures at the same wavelength. These data are consistent with previous results (14 ns and 0.14

ns) obtained at 43°C by Munro et al.<sup>23</sup> The longer value is usually associated with the overall rotation of the protein in solution, whereas the shorter component is attributed to the internal motion of the single Trp in HSA. By  $f_L$  value, it is possible to estimate the angular displacement responsible for shorter motion, according to the formula<sup>24</sup>:

$$\cos^2\theta = (2f_L + 1)/3$$

By this formula, it is possible to calculate a rotation angle of about 37° for Trp in HSA at 37°C. NOEA induced no

modifications in rotational correlation times and in the rotation angle. The anisotropy decay of BSA at 37°C is analyzed using two rotational correlation times, 15.1 ns and 0.24 ns, with  $f_L$  0.41. The limiting anisotropy  $r_0$  is fixed at the experimental value 0.31. NOEA does not significantly modify both rotational correlation times and  $f_L$  (16.1 ns, 0.17 ns and 0.45, respectively). The anisotropy decay of BSA at 37°C is analyzed using two rotational correlation times, 15.1 ns and 0.24 ns, showing no significant differences with HSA. No changes of these parameters are induced by NOEA. Control experiments performed in the presence of increasing ethanol concentrations (up to 50 mM) showed no ethanol-induced modification of fluorescence decay features in both BSA and HSA (data not shown).

### ANS Steady-State Fluorescence

The binding of NOEA to albumins was studied also by the steady-state fluorescence of ANS, whose quantum yield is significantly increased after binding to many proteins.<sup>25</sup> This amphiphilic probe is almost completely not fluorescent in water, whereas its fluorescence increases as consequence of the interaction with hydrophobic sites on a protein. Recent results demonstrated that the average binding constant for ANS-BSA complex was large ( $10^4$ – $10^5$  mol<sup>-1</sup>) and the number of binding sites measurable by fluorescence was at least 3.<sup>26,27</sup> In the present work, BSA titration by NOEA increases ANS fluorescence intensity ( $\lambda_{ex} = 350$  nm) at each concentration used (maximum increase  $\approx 12\%$ ), suggesting an increased binding of the probe to BSA (Fig. 3B). Figure 3D shows the emission spectra of the ANS-BSA complex obtained by excitation at 295 nm, in the presence of increasing concentrations of NOEA. These spectra are characterized by two emission bands with maxima centered at wavelengths corresponding to Trp and ANS emission, respectively. The fluorescence intensity of the ANS band increases with ligand concentration, whereas the opposite is observed for the Trp band. This complex behavior is owing to energy transfer from Trp to ANS, which is more probable within a distance of 2.3 nm.<sup>25</sup> The maximum increase in ANS fluorescence in the spectra obtained with  $\lambda_{ex} = 295$  nm, was 17%.

ANS fluorescence was studied also in the complex ANS-HSA. Previous studies<sup>28</sup> demonstrated that this protein is characterized by one or two fluorescent binding sites, depending on the ANS/albumin molar ratio. On HSA, the ANS binding site with larger affinity was identified on subdomain IIIA ( $K_{ass} = 0.87 \times 10^6$  mol<sup>-1</sup>), whereas a lower affinity site was identified on subdomain IIA. In our experimental conditions, ANS (ANS/albumin molar ratio = 0.65) is linked only to the subdomain IIIA.<sup>29</sup> Figure 3A shows the emission spectra of the ANS-HSA complex obtained by excitation at 350 nm. Increasing concentrations of NOEA induce a red shift and a decrease in ANS fluorescence intensity. The maximum decrease obtained at 29  $\mu$ M NOEA concentration was 10%. These results could indicate that NOEA and ANS compete for the same binding site, although other explanations could be

possible, such as a decreased hydrophobicity at this site<sup>27</sup> or a change in the rigidity of the fluorophore environment.<sup>25</sup> Figure 3C shows the emission spectra of the ANS-HSA complex obtained by excitation at 295 nm, in the presence of increasing concentrations of NOEA. A red shift and a small decrease in ANS fluorescence emission is measurable, whereas no changes in Trp spectrum are evident.

### Circular Dichroism

Far and near UV C.D. measurements were performed on BSA and HSA samples in the absence and in the presence of increasing amounts of NOEA at room temperature. Far C.D. spectra for both proteins show only small modifications induced by NOEA at the higher NOEA/albumin molar ratio tested  $R = 7.5$  (data not shown). Also, the near UV C.D., which gives indications on the tertiary structure of proteins, shows only small changes on both albumins in the range  $R = 4.5$ – $7.5$  (data not shown).

### 3D-Space-Filling Modeling

Figure 4 shows a 3-D space-filling model. On the basis of experimental data, the NOEA molecule was docked to the higher affinity fatty acid binding site, in the domain IIIA involving residues Pro 384, Leu 387, Ile 388, Phe 395, Leu 407, Leu 430, Val 433, Met 446, Ala 449, Leu 453. This binding site is near the residue Trp 214 in HSA (3 Å). The ligand was oriented into the binding site and its orientation was checked to ensure the lack of unacceptable steric interactions between the ligand and the protein. The protein coordinates were obtained from the Protein Data Bank.<sup>38</sup> The complex ligand-protein was then allowed to relax and to reach the lowest energy.

## DISCUSSION

The fluorescence features of Trp residues are largely used to study structural and dynamic characteristics of proteins, and they are considered useful to study binding of extrinsic molecules to albumins.<sup>13,14,30</sup> Trp fluorescence emission maximum is usually related to the polarity of its environment: a red shift is expected when the fluorescent molecule becomes more exposed to a polar solvent. The fluorescence emission intensity is linked to a variety of phenomena, such as the exposure to polar solvents, quenching, excited state reactions. The blue shift owing to exposure to less polar solvents is usually associated with an increase in fluorescence intensity. A Trp  $\lambda_{em}$  blue shift, associated with a fluorescence intensity decrease, was induced by the binding of most long-chain fatty acids to BSA<sup>27</sup> (and references cited therein). This was interpreted as not due to Förster energy transfer, but rather to a conformational effect.<sup>31</sup>

In this work, the NOEA-induced  $\lambda_{em}$  blue shift, measured on both albumins, suggests a decrease in the environment polarity of Trp-214 in HSA and at least one of the indole rings present in BSA. Although direct quenching by NOEA was excluded (see Results), the fluorescence intensity decrease could be, at least partially, related to structural and/or conformational changes, which may influence

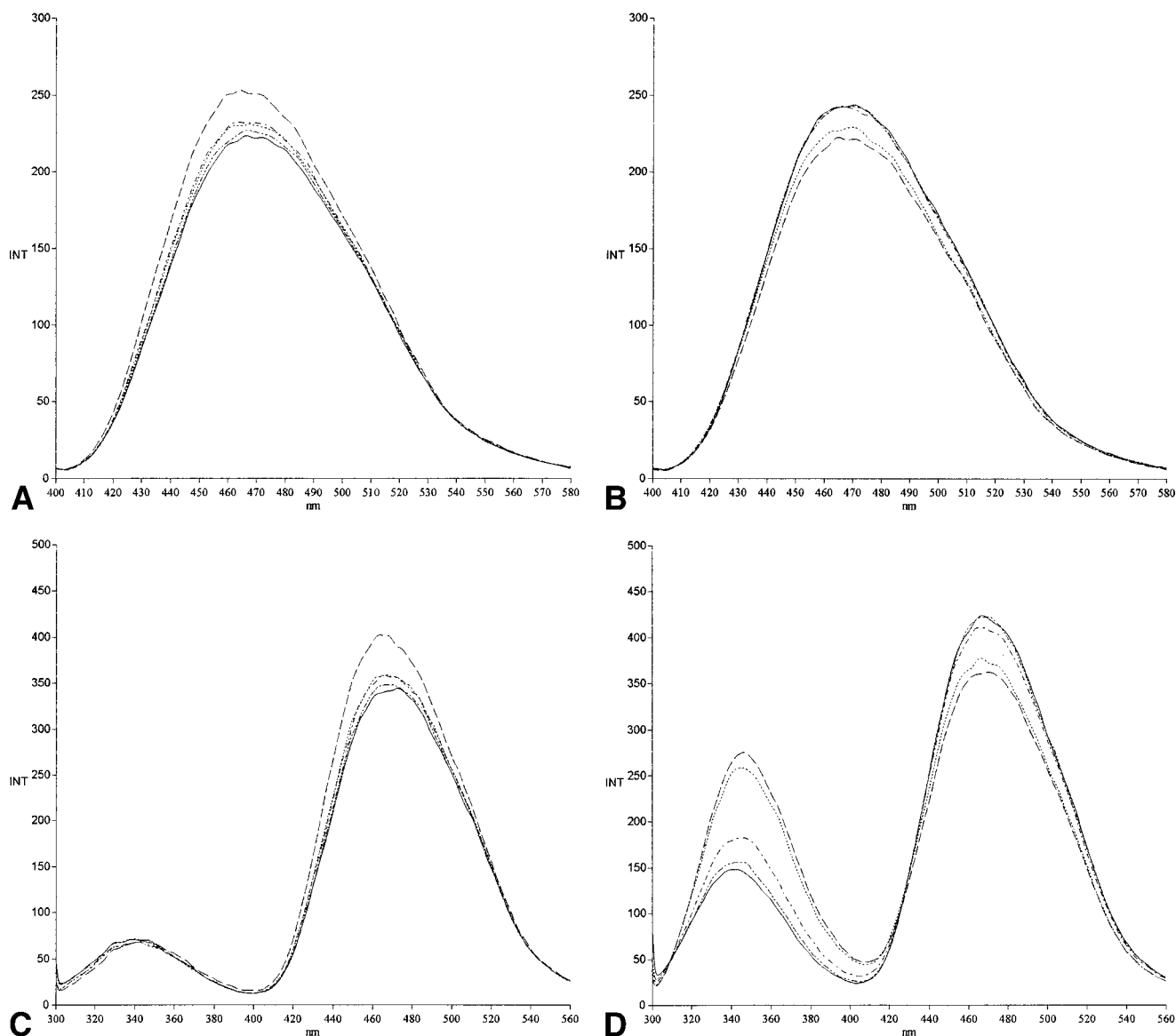


Fig. 3. Effect of increasing NOEA concentrations on ANS fluorescence spectra of ANS-HSA (panels A and C) and ANS-BSA (panels B and D) complexes. In Figure A and B, excitation wavelength = 350 nm, in panels C and D excitation wavelength = 295 nm. ANS final concentration

was 1.8  $\mu\text{M}$ ; both proteins were 190  $\mu\text{g/ml}$ . (---) Control; (···) 2.9  $\mu\text{M}$  NOEA; (-·-·-) 8.8  $\mu\text{M}$  NOEA; (·-·-·) 17.5  $\mu\text{M}$  NOEA; (—) 29.2  $\mu\text{M}$  NOEA. Spectra were recorded at 37°C.

the interaction of Trp residues with their neighbors, affecting the possibility of quenching and/or excited state reactions with other moieties present on the polypeptide chain. Assuming that Trp-214 in HSA and Trp-212 in BSA show similar fluorescence behavior, the measured differences in steady-state data obtained for these proteins are likely owing to Trp-134. However, C.D. spectra indicate that acylethanolamine binding is not associated with substantial structural changes, because the secondary and tertiary structures of both proteins are only slightly affected. This result is in agreement with previous works, showing no changes in the protein secondary structure induced by the linkage of different ligands.<sup>30,32,33</sup> Trp steady-state fluorescence demonstrates that both albu-

mins are affected by  $\mu\text{molar}$  concentrations of NOEA. However, the calculated  $K_a$  for the two proteins are significantly different, indicating that the binding sites measurable by Trp fluorescence changes in HSA (likely located in the hydrophobic environment of Trp-214) are characterized by a larger affinity for the long oleic acyl chain of NOEA than the binding sites near Trp 134 in BSA. Time-resolved fluorescence measurements can give information about the conformational heterogeneity of proteins. Many factors, including exposure to water molecules, to many other moieties intrinsic to protein structure and/or excited state processes can modify the Trp fluorescence lifetime, which can vary by more than a factor of 100 in different polypeptides.<sup>34</sup> Trp emission decay is satisfac-



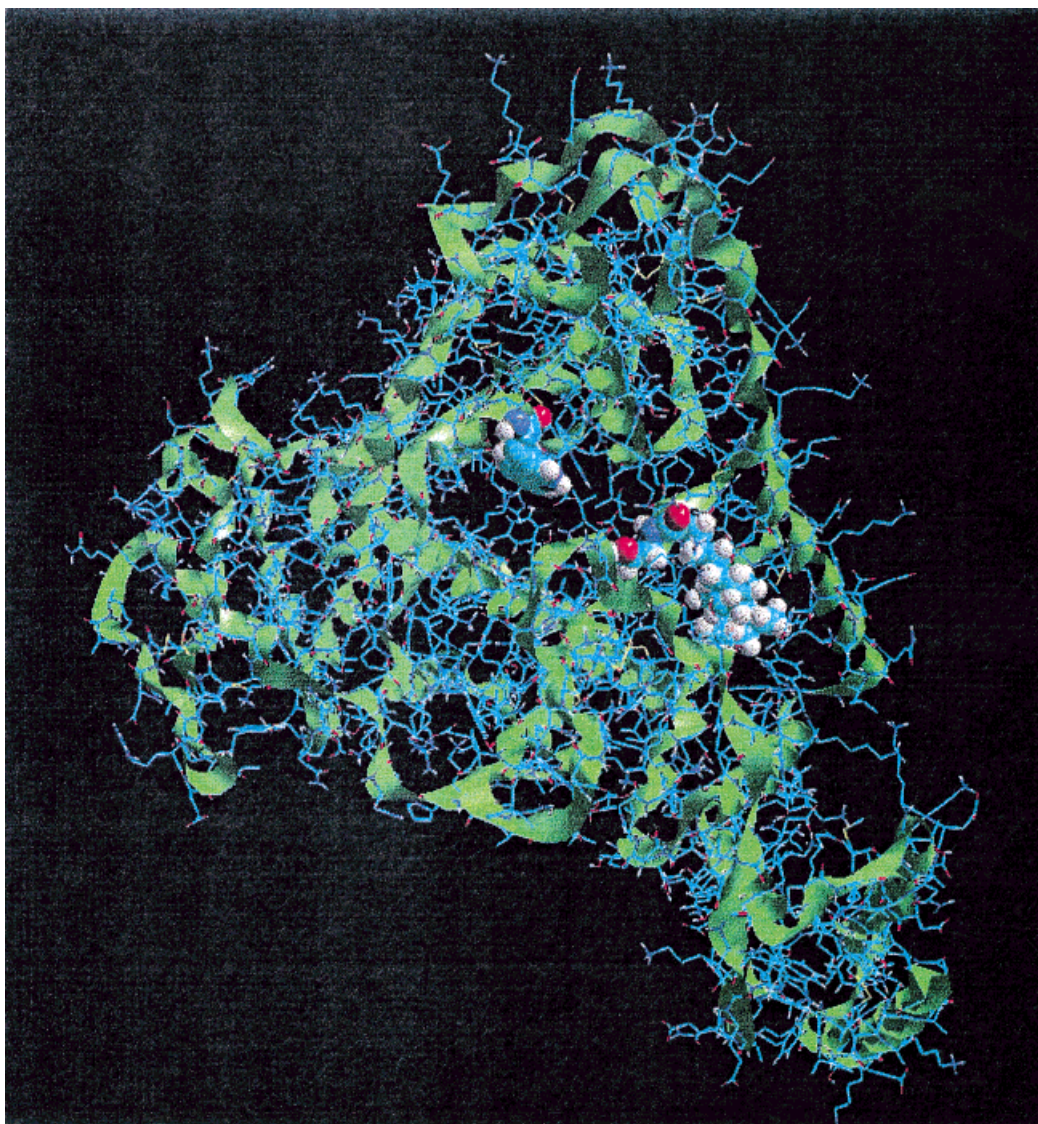


Fig. 4. 3-D space-filling model of HSA complexed with NOEA. The residue Trp-214 and the NOEA molecule are shown in evidence. The protein coordinates were obtained from the Protein Data Bank.<sup>38</sup>

torily described by several exponential components, usually associated with different amino acid residues. However, a complex fluorescence decay, owing to conformational heterogeneity, can be observed also in single fluorophore-containing proteins.<sup>34</sup> Complex decays of Trp fluorescence were described in terms of continuous lifetime distributions.<sup>15</sup> Gratton and co-workers<sup>15, 35, 36</sup> demonstrated that, in single Trp proteins, the lifetime distribution width is related to the flexibility of the protein structure, thus determining the heterogeneity of Trp environments experienced during its excited state. It was suggested that the width of lifetime distribution, in single Trp proteins, is related to the extent of motion of the fluorophore (namely, decreasing as the rate of motion increases) and/or to a larger number of microenvironments experienced by Trp (namely, increasing when this number is increased).<sup>15, 35, 36</sup> The presence of several Trp residues increases the complex-

ity of the model. However, it is known that the single Trp-214 in HSA and Trp-212 in BSA are located in similar microenvironments,<sup>10</sup> and it is generally assumed that the fluorescence emission of these amino acid residues is affected to the same extent by ligands.<sup>14, 30</sup> Because BSA fluorescence decay is a weighted average of Trp-134 and Trp-212 decays, the possible differences between data analysis of BSA and HSA can give indications on Trp-134 residue.

Results obtained suggest that only Trp-214 lifetime (or Trp-212 in BSA) is affected by NOEA, excluding the presence of binding sites with similar affinity near Trp-134. Trp lifetime decrease (Table I) is not related to an increased exposure to the solvent, because the blue shift in the steady-state emission spectra indicate a lower polarity in the fluorophore environment (Fig. 1). Although a direct quenching by NOEA was excluded, a decrease in lifetime

value is probably related to conformational changes, modifying phenomena such as dynamic quenching, and/or to excited state processes owing to moieties present in the polypeptide. Data could indicate a NOEA-induced conformational change of HSA in the domain containing Trp-214, affecting distances among amino acids residues (including Hys, Cys, Pro, Arg, and peptide bond), which are capable of quenching Trp fluorescence. However, the possibility that the part of peptide chain containing Trp-214 (loop 4) is not directly involved in NOEA binding is suggested by the unmodified value of Gaussian distributional width, indicating that there are no changes in the heterogeneity of Trp environment. These conclusions are suggested also by the unmodified local Trp motions and the unmodified rotational angle for this residue in HSA (about 36°). Moreover, this NOEA concentration induces no change in the protein shape. Data presented suggest that, at the NOEA concentrations tested, the binding of acylethanolamine could induce a remodeling in the relative position of domains, but not in their structure.

The principal hydrophobic binding regions on HSA and BSA are located in subdomains IIA and IIIA,<sup>10,11,37</sup> whereas Domain I, characterized by a strong net negative charge<sup>10</sup> was shown to offer the proper binding sites to cationic ligands, such as Ca<sup>2+</sup> and Zn<sup>2+</sup> ions.<sup>10</sup> Many hydrophobic ligands are known to link preferentially in the binding cavity in subdomain IIIA. For both HSA and BSA, it was suggested that the primary fatty acid binding site is in the middle of third domain, dependent for its apolar nature on tertiary folding of the largely helical loops 7–9.<sup>10</sup> The second fatty acid binding site was identified in loop 6, forming a hydrophobic pocket in the region between domains II and III.<sup>10</sup> A three-dimensional atomic model of albumin showed a hydrophobic channel, in the middle of domain III, having dimensions well tailored to match an extended C<sub>16</sub>-C<sub>20</sub> acyl chain.<sup>10</sup> These properties suggest that the C<sub>18</sub> oleic acyl chain of NOEA could interact primarily at these sites, similarly to fatty acids.

Our data obtained using Trp fluorescence can be in agreement with this hypothesis, because, in HSA, Trp-214 is localized in IIA subdomain, but it participates in additional hydrophobic packing interactions between IIA and IIIA interface.<sup>11</sup> Modifications in this protein region could easily affect Trp fluorescence.

The fluorescent probe ANS can be useful to verify the possible modifications induced by NOEA on subdomain IIIA of HSA. Previous studies demonstrated that ANS, in the concentration used in this work, is linked only to subdomain IIIA on HSA.<sup>28,29</sup> ANS fluorescence was used to monitor ligand binding of this subdomain,<sup>28,29</sup> by correlating a decreased ANS intensity to successive displacements of the probe from its binding site. In our experiments, the hypothesis of ANS displacement seems not to be consistent with energy-transfer measurements (Fig. 3A), because a NOEA-induced intensity decrease in ANS emission is not associated with changes in Trp spectra. These results suggest a decreased energy-transfer efficiency, which could be because of a longer donor-acceptor distance and/or to conformational changes modifying the

rigidity of the fluorophore environment.<sup>25</sup> Also, results obtained by Monte Carlo procedure suggest that NOEA localizes into the same fatty acid first binding site with the same orientation. This is the only one that minimizes all the negative and destabilizing interactions between the NOEA and the albumin. Also, the NOEA interaction with BSA was studied by ANS fluorescence. It was shown that the number of ANS binding sites measurable by fluorescence on BSA is  $2.82 \pm 0.08$ <sup>26</sup> ( $K_a = 2.06 \pm 0.06 \times 10^4 \text{ mol}^{-1}$ ). Moreover, it is known that ANS and the 3rd, 4th, and 5th fatty acids bound to BSA share the same binding regions<sup>26</sup> (and references cited therein), whereas up to 2 mol of fatty acids for mole of BSA do not affect ANS binding to BSA.<sup>26</sup> Our experiments suggest an ANS greater interaction with the protein, which could expose a larger number of hydrophobic residues to solvent, in the presence of NOEA. Moreover, the increased ANS fluorescence intensity could be owing to the formation of new ANS binding sites in the Trp-134 environment. Alignment of the known sequences of HSA and BSA showed an 80% homology between these proteins. However, this agreement is close in all loops, except loop-3, containing Trp-134.<sup>10</sup> This lower homology could be the cause of the different fluorescence intensity behavior of the ANS-HSA and ANS-BSA complexes, excited at 350 nm. The fluorescence of ANS-BSA complex indicates that NOEA and ANS do not share the same binding sites, because a decrease in ANS intensity was expected in this case. Moreover, these data indicate that NOEA does not occupy, on BSA, the same binding sites of the 3rd, 4th, and 5th fatty acids, which are known to be linked, with relatively low affinities, to proper clefts and pockets on the protein.

## CONCLUSIONS

Our data suggest that NOEA binds with high affinity to HSA and BSA, modifying their conformational features. In both proteins, NOEA molecules are linked with higher affinity to hydrophobic sites near Trp-214 (or 212). Moreover, ANS fluorescence data and BSA-HSA spectra of Trp-134 support the hypothesis of the presence of other NOEA binding sites on BSA, affecting Trp-134 environment. Similar binding sites cannot be detected in HSA because Trp-134 is absent. N-acyl ethanolamines, and their precursors NAEs, are formed in tissues as response to cellular injury,<sup>1,6</sup> and are supposed to serve as a cytoprotective response.<sup>6</sup> Moreover, N-acyl ethanolamines are known to possess some pharmacological actions: in fact, some NAEs are reported to have anti-inflammatory, anti-anaphylactic, and anti-serotonin activity.<sup>1</sup> Besides, it was shown that NOEA inhibits thrombin-induced human platelet aggregation.<sup>1</sup> The pharmacological effects of NAEs can be affected by their absorption, circulation, and tissue distribution.<sup>1</sup> Because albumins are known to contribute significantly to transport, distribution, and metabolism of many exogenous and endogenous ligands, a characterization of NAE-albumin binding can help to elucidate the mechanism of their biological effects and their possible use as therapeutic agents. Moreover, the characteristics of NAEs binding sites on albumin could be proper models for



the understanding of structural and chemical features of binding sites on proteins that are known to interact with these molecules, such as cannabinoid receptors, which are activated by some NAEs, such as anandamide and palmitoylethanolamide.<sup>4,39,40</sup> Other experiments are in progress in this laboratory to increase the characterization of NAEs interactions with albumins.

### ACKNOWLEDGMENTS

We wish to thank Dr. Theodore Hazlett for his assistance with the time-resolved measurements, which were performed at the Laboratory for Fluorescence Dynamics (LFD), University of Illinois at Urbana-Champaign. This work was supported by a grant from M.U.R.S.T 60% to G.Z. and CNR fund 98.00416CT04 to E.B.

### REFERENCES

- Schmid HHO, Schmid PC, Natarajan V. N-acylated glycerophospholipids and their derivatives. *Prog Lip Res* 1990;29:1-43.
- Di Marzo V, Fontana A, Cadas H, Schinelli S, Cimino G, Schwartz JC. Formation and inactivation of endogenous cannabinoid anandamide in central neurons. *Nature (London)* 1994;346:561-564.
- Ambrosini A, Bertoli E, Mariani P, Tanfani F, Wozniak M, Zolese G. N-acylethanolamines as membrane topological stress compromising agents. *Biochim.Biophys.Acta* 1993;1148:351-355.
- Facci L, Dal Toso R, Romanello S, Buriani A, Skaper SD, Leon A. Mast cells express a peripheral cannabinoid receptor with differential sensitivity to anandamide and palmitoylethanolamide. *Proc Natl Acad Sci USA* 1995;92:3376-3380.
- Skaper SD, Buriani A, Dal Toso R, Petrelli L, Romanello S, Facci L, Leon A. The ALLamide palmitoylethanolamide and cannabinoids, but not anandamide, are protective in a delayed postglutamate paradigm of excitotoxic death in cerebellar granule neurons. *Proc Natl Acad Sci USA* 1996;93:3984-3989.
- Hansen HS, Lauritzen L, Moesgaard B, Strand AM, Hansen HH. Formation of N-acyl-phosphatidylethanolamines and N-acetylethanolamines: proposed role in neurotoxicity. *Biochem Pharmacol* 1998;55:719-725.
- Pardridge WM. Plasma protein-mediated transport of steroid and thyroid hormones. *Am J Physiol* 1987;252:157-164.
- Schnitzer JE, Carley WW, Palade GE. Albumin interacts specifically with a 60-kDa microvascular endothelial glycoprotein. *Proc Natl Acad Sci USA* 1988;85:6773-6777.
- Carter DC, He X-M, Munson SH, Twigg PD, Gernert KM, Broom MB, Miller TY. Three-dimensional structure of human serum albumin. *Science* 1992;244:1195-1198.
- Peters T, Jr. Serum albumin. *Adv Protein Chem* 1985;37:161-245.
- He XM, Carter DC. Atomic structure and chemistry of human serum albumin. *Nature* 1992;358:209-215.
- Helms MK, Petersen CE, Bhagavan NV, Jameson DM. Time-resolved fluorescence studies on site-directed mutants of human serum albumin. *FEBS Lett* 1997;408:67-70.
- Johansson JS, Eckenoff RG, Dutton L. Binding of halothane to serum albumin demonstrated using tryptophan fluorescence. *Anesthesiology* 1995;83:316-324.
- Moriyama Y, Ohta D, Hachiya K, Mitsui Y, Takeda K. Fluorescence behavior of tryptophan residues of bovine and human serum albumins in ionic surfactant solutions: a comparative study of the two and one tryptophan(s) of bovine and human albumins. *J Protein Chem* 1996;15:265-272.
- Alcala JR, Gratton E, Prendergast F. Resolvability of fluorescence lifetime distributions using phase fluorometry. *Biophys J* 1987;51:587-604.
- Goodsell DS, Olson AJ. Automated docking of substrates to protein by simulated annealing. *Proteins: Structure, Function Genetics* 1990;8:195-202.
- Weiner SJ, Kollman PA, Case DA, Singh UC, Ghio C, Alagona G, Profeta S, Weiner P. A new force field for molecular mechanical simulation of nucleic acids and proteins. *J Am Chem Soc* 1984;106:765-784.
- Mohamadi F, Richards NGJ, Guida WC, Liskamp R, Lipton M, Caufied C, Chang G, Hendrickson T, Still WC. MacroModel—an integrated software system for modeling organic and bioorganic molecules using molecular mechanics. *J Comp Chem* 1990;11:440-467.
- Ehrhardt MR, Erjman L, Weber G, Wand AJ. Molecular recognition by calmodulin: pressure-induced reorganization of a novel calmodulin-peptide complex. *Biochemistry* 1996;35:1599-1605.
- Marzola P, Gratton E. Hydration and protein dynamics: frequency domain fluorescence spectroscopy on proteins in reverse micelles. *J Phys Chem* 1991;95:9488-9495.
- Zolese G, Giambanco I, Curatola G, De Stasio G, Donato R. Time-resolved fluorescence of S-100a protein in the absence and presence of calcium and phospholipids. *Biochim Biophys Acta* 1993;1162:47-53.
- Zolese G, Giambanco I, Curatola G, Staffolani R, Gratton E, Donato R. Time-resolved fluorescence of S-100a protein: effect of Ca<sup>2+</sup>, Mg<sup>2+</sup> and unilamellar vesicles of egg phosphatidylcholine. *Cell Calcium* 1996;20:465-474.
- Munro I, Pecht I, Stryer L. Subnanosecond motions of tryptophan residues in proteins. *Proc Natl Acad Sci USA* 1979;76:56-60.
- Lakowicz JR. Principles of fluorescence spectroscopy. New York: Plenum Press, 1986.
- Slavik J. Anilino-naphthalene sulfonate as a probe of membrane composition and function. *Biochim Biophys Acta* 1982;694:1-25.
- Avdulov NA, Chochina SV, Daragan VA, Schroeder F, Mayo KH, Wood WG. Direct binding of ethanol to bovine serum albumin: a fluorescent and <sup>13</sup>C NMR multiplet relaxation study. *Biochemistry* 1996;35:340-347.
- Cardamone M, Puri NK. Spectrofluorimetric assessment of the surface hydrophobicity of proteins. *Biochem J* 1992;282:589-593.
- Bagatolli LA, Kivatinitz SC, Aguilar F, Soto MA, Sotomayor P, Fidelio GD. Two distinguishable fluorescent modes of 1-anilino-8-naphthalenesulfonate bound to human albumin. *J Fluorescence* 1996;6:33-40.
- Bagatolli LA, Kivatinitz SC, Fidelio GD. Interaction of small ligands with human serum albumin IIIA subdomain. How to determine the affinity constant using an easy steady-state fluorescent method. *J Pharm Sci* 1996;85:1131-1132.
- Johansson JS. Binding of the volatile anesthetic chloroform to albumin demonstrated using tryptophan fluorescence quenching. *J Biol Chem* 1997;272:17961-17965.
- Sklar LA, Hudson BS, Dimoni RD. Conjugated polyene fatty acids as fluorescent probes: binding to bovine serum albumin. *Biochemistry* 1977;16:5100-5108.
- Laskowski RA, Luscombe NM, Swindells MB, Thornton JM. Protein clefts in molecular recognition and function. *Protein Sci* 1996;5:2438-2452.
- Kurumbail RG, Stevens AM, Gierse JK, McDonald JJ, Stegeman RA, Pak JY, Gildehaus D, Miyashiro JM, Penning TD, Seibert K, Isakson PC, Stallings WC. Structural basis for selective inhibition of cyclooxygenase-2 by anti-inflammatory agents. *Nature* 1996;384:644-648.
- Beechem JM, Brand L. Time-resolved fluorescence of proteins. *Annu Rev Biochem* 1985;54:43-71.
- Gratton E, Silva N, Mei G, Rosato N, Savini I, Finazzi-Agrò A. Fluorescence lifetime distribution of folded and unfolded proteins. *Int J Quantum Chem* 1992;42:1479-1489.
- Silva N, Mei G, Gratton E. Proteins fluorescence and conformational substates: the dynamics of human superoxide dismutase. *Commun Mol Cell Biophys* 1994;8:217-242.
- Fleury F, Kudelina I, Nabiev I. Interactions of lactone, carboxylate and self-aggregated forms of camptothecin with human and bovine serum albumins. *FEBS Lett* 1997;406:151-156.
- Curry S, Mandelkow H, Brick P, Franks N. Crystal structure of human serum albumin complexed with fatty acid reveals an asymmetric distribution of binding sites. *Nat Struct Biol* 1998;5:827-835.
- Bisogno T, Maurelli S, Melck D, De Petrocelli L, Di Marzo V. Biosynthesis, uptake, and degradation of anandamide and palmitoylethanolamide in leukocytes. *J Biol Chem* 1997;272:3315-3323.
- Di Marzo V. 'Endocannabinoids' and other fatty acid derivatives with cannabimimetic properties: biochemistry and possible physiopathological relevance. *Biochim Biophys Acta* 1998;1392:153-175.